

Quantifying the Stabilizing Energy of the Intraprotein Hydrogen Bond Due to Local Mutation

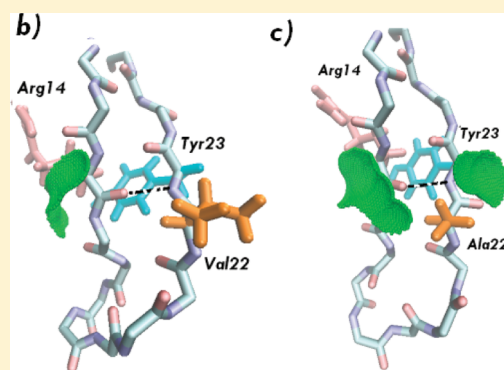
Chang G. Ji^{*,†,‡} and John Z. H. Zhang^{*,†,‡,§}

[†]State Key Laboratory of Precision Spectroscopy, Department of Physics, East China Normal University, Shanghai 200062, China

[‡]Institute of Theoretical and Computational Science, Institutes for Advanced Interdisciplinary Research, East China Normal University, Shanghai 200062, China

[§]Department of Chemistry, New York University, New York, New York 10003, United States

ABSTRACT: MD simulation of the WW domain of PIN based on a dynamically adjusted polarized protein-specific force field from quantum fragment calculations is carried out in both wild and VAL22ALA mutant states. The result shows that the geometry of the Arg14-TYR23 hydrogen bond is conserved upon mutation of VAL22 to ALA. However, the electrostatic energy of this hydrogen bond in the mutant is found to be 0.6 kcal/mol weaker than in the wild state, in close agreement with the experimentally measured upper limit of 1.2 kcal/mol. Analysis shows that the weakened energy of this hydrogen bond in the mutant is due to its dynamically changed polarization resulting from an altered local electrostatic environment near the hydrogen bond which becomes more exposed to the solvent than in the wild.



The hydrogen bond is one of the most important structural elements in folded proteins¹ and has attracted much experimental and theoretical interest.^{2,3} One of the central issues in its current research is whether hydrogen bonds energetically act as a liability or an asset in protein folding.³ Conclusions derived from different experiments often disagree. Early experiments based on dimerization of *N*-methyl acetamide (NMA) monomers showed that hydrogen bond formation is an energetically disfavored process⁴ in an aqueous environment. Based on their continuum electrostatic calculations,^{5–7} Anbelj and Baldwin suggested that simple NMA based experiments may not act as a model system for studying energetics of hydrogen bonds in protein folding. Systematic studies by Baldwin and co-workers showed, however, that a short poly(alanyl) peptide can form a stable helix in water, implying that the hydrogen bond contributes to the stability of the protein.⁸ On the other hand, theoretical studies by Honig and co-workers concluded that the hydrogen bond does not contribute to helix stability due to a large desolvation penalty in hydrogen-bond formation.^{9–11} Thus, the contribution of hydrogen bonding to protein stability remains unclear.

It was shown that contribution of a hydrogen bond to protein stability depends on the polarity of hydrogen bond's microenvironment.^{12–14} A recent study by Gao et al has shown that hydrogen bonds are much stronger in a nonpolar microenvironment than in a polar microenvironment.¹⁵ The effect was quantitatively measured with double mutation experiments. However, mutations may be accompanied by structural changes, which can confound the experimental results. Thus, the molecular origins of a macroscopically observed difference in hydrogen bond strength are difficult to access. On the other hand, computational studies

can quantify individual interaction elements directly, without introducing any structural perturbation. Here we investigate the strength of hydrogen bonds under different electrostatic environments through quantum chemical calculation and MD simulation.¹⁶ Since standard force fields are nonpolarizable and unable to describe the polarization effect,¹⁷ we computed the polarized protein-specific charge (PPC) for MD simulations in both states to account for the polarization effect. PPC is derived from a fragment quantum electronic structure calculation of protein in solvent.¹⁸ The polarization effect is explicitly included in the quantum chemistry calculation based on which RESP atomic charges are fitted.^{19–21} Here we focus on a particular backbone hydrogen bond in the WW domain of PIN, which was studied experimentally by Gao et al.¹⁵ We study the dynamic and energetic properties of this hydrogen bond in different electrostatic environments achieved through mutation.

The hydrogen bond between CO of Arg14 and NH of TYR23 is studied in this work. TYR23's neighboring residue VAL22 has a large side chain. As shown in Figure 1, VAL22 and other nearby side chains help create a nonpolar microenvironment for this hydrogen bond and shield it from the solvent. Compared with the V22A mutant, the solvent accessible surface around the hydrogen bond in the wild-type protein is sharply reduced due to the large side chain of V22 (see Figure 1). Following the experimental approach, the microenvironment for this hydrogen bond was modeled through mutation from VAL22 to ALA.

Received: June 23, 2011

Revised: September 13, 2011

Published: September 14, 2011

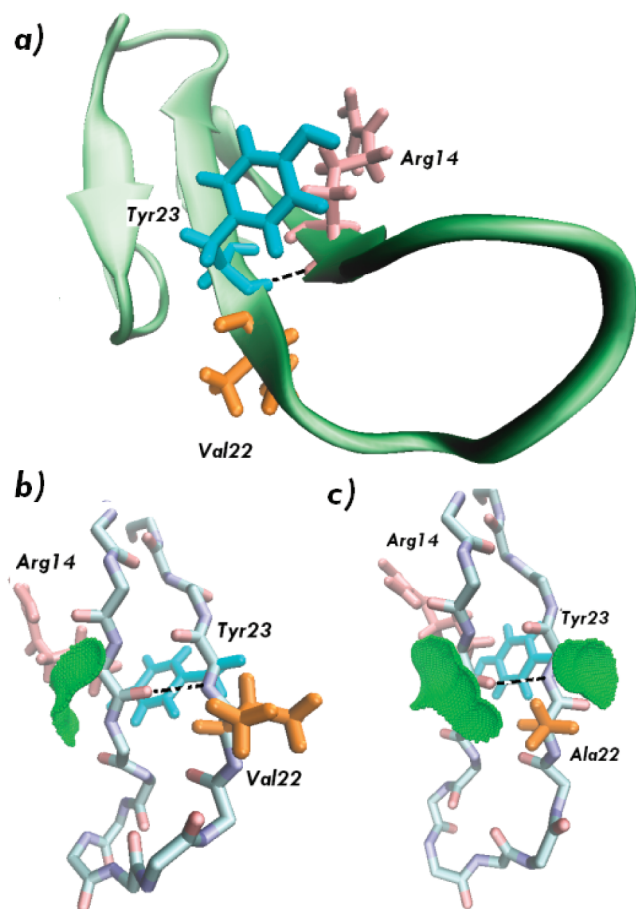


Figure 1. Structure of Pin WW domain with a hydrogen bond formed between CO of Arg14 and NH of Tyr23 (Picture was generated from crystal structure. PDB ID:1PIN). (a) Cartoon representation of the wild state with the hydrogen bond represented by the black dashed line. (b) Solvent accessible surface around this hydrogen bond is represented by green surface in wild type. (c) Same as in panel b but for the V22A mutant (truncate V22 side chain of wild-type crystal structure directly).

In this study, a 20 ns MD simulation was performed and the trajectory was analyzed. The dynamics simulation is carried out with a time step of 1 fs. PPC was updated every 40 ps to properly account for the dynamic fluctuation of the structure. In principle, updating the atomic charge at every time step during the MD simulation should be more desirable. However, such frequent updating is computationally too expensive due to the cost of quantum calculations to generate structure-specific PPC for the protein. Based on our computational test (see the Computational Methods section below), the 40 ps updating is found to give very reasonable results. The MD trajectory was saved every 2 ps, resulting in 10 000 snapshots for further analysis in each simulation.

The geometry of the Arg14-Tyr23 hydrogen bond is not affected by the mutation as can be seen from the dynamic distribution of hydrogen bond length of the wild and mutated WW domain in Figure 2a. Also, the average angle of the hydrogen bond differs by only about 1° between wild and mutant states. The result shows that V22A mutation does not bring extra structural change to the original hydrogen bond. Thus our MD result supports the experimental hypothesis of structural conservation of this hydrogen bond in V22A mutation.¹⁵

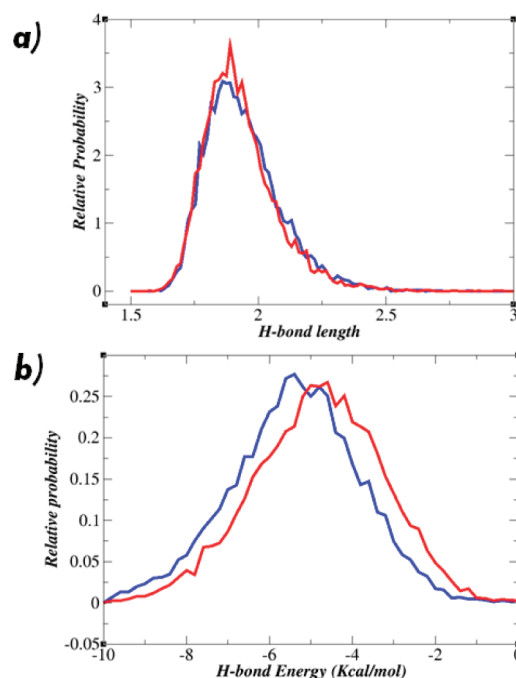


Figure 2. (a) Distribution of hydrogen bond length from MD simulation. (b) Distribution of hydrogen bond strength during MD simulation (red:V22A mutant, blue:wild).

The strength of the hydrogen bond is determined by direct nonbonding electrostatic interactions between NH and CO groups. In the standard AMBER or CHARMM force fields, atomic charges are fixed during the simulation and they are the same in both wild type and mutant. Thus such charge models are incapable of detecting energy change of this hydrogen bond which arises purely from the polarization effect, not structural change as shown in Figure 2a.

Figure 2b shows the distribution of electrostatic energy of the hydrogen bond during MD simulation. It is clear that the energy of this hydrogen bond is different in two systems although their geometries remain essentially the same. This hydrogen bond is 0.6 kcal/mol stronger in the wild-type protein (H-bond energy = -5.5 kcal/mol) than in the V22A mutant (H-bond energy = -4.9 kcal/mol), presumably due to the difference in the electronic polarization of the hydrogen bond under different microenvironments. Since VAL22 has a large hydrophobic side chain, it can shield the hydrogen bond away from the solvent (water) molecules. This is demonstrated in Figure 3 in which the distribution of water molecules near (within 3.4 Å) the hydrogen bond in the first solvation shell is plotted for both wild and mutated states. Our calculation gives an average number of 0.9 water molecules within the 3.4 Å of the hydrogen bond in the V22A mutant vs 0.6 in the wild-type protein. Our computational result can be understood from Figure 1 which shows that the hydrogen bond is accessible to more solvent molecules in the V22A mutant than in the wild-type protein. The difference in H-bond energy observed between the wild-type protein and the V22A mutant in the current study is significant because it accurately predicts the experimental observations of Gao et al in which they found an upper limit of 1.2 kcal/mol in energy difference between the wild and mutant.¹⁵ The overlap in the probability curves (see Figure 2b) simply reflects the dynamic nature of the H-bond as a function of time during the simulation (see Figure 4).

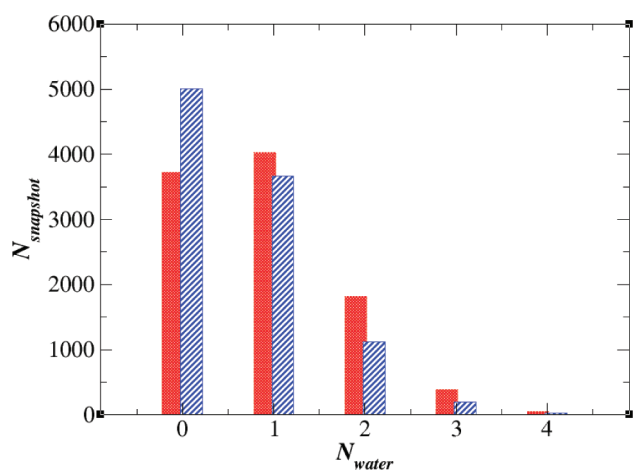


Figure 3. Histogram for the number of water molecules around the hydrogen bond in the first solvation shell (striped blue: wild type, red: V22A mutant).

Although the energy difference of 0.6 kcal/mol in a single hydrogen bond may not seem very large, considering that there may be hundreds of hydrogen bonds in a functional protein²² and the collective effect could be significant. With respect to folding, the free energy difference between folded and the unfolded states is often only a few kcal/mol for most of the proteins.^{23,24} Thus accurate accounting of each hydrogen bond's strength in its proper electrostatic environment is very important in understanding the critical role of hydrogen bond in stabilizing protein's three-dimensional structure and other important biological processes.

One should note that, because the hydrogen bond is dynamic (hydrogen bond geometry fluctuates in time), it is necessary to perform statistical averaging over MD trajectories in order to correctly differentiate such small energy difference (less than 1 kcal/mol) between the wild and mutant. Figure 4 shows the fluctuation of this H-bond energy resulting from the dynamic motion of the hydrogen bond throughout the simulation time.

It is also informative to compare the result from MD simulation under standard (nonpolarizable) force field. By using the AMBER force field, the calculated electrostatic energy of this hydrogen bond is relatively weaker (−2.8 kcal/mol) in both wild and mutant, obviously due to the lack of electronic polarization. Under AMBER force field, the atomic charges remain the same in both wild and mutant states, irrespective of the specific micro-environment of the hydrogen bond.

Electrostatic interaction is the dominant element in hydrogen bonded systems. The CO and NH bonds are polarized in the formation of hydrogen bond. These two dipoles polarize each other and thus energetically strengthen the hydrogen bond. Proteins are not homogeneous,²⁵ therefore the polarization of the hydrogen bond is affected by the specific local electrostatic environment (i.e., the polarization of a buried hydrogen bond should be different from that of a solvent-exposed hydrogen bond). Thus their contribution to folding energy should be different. Accurate description of these hydrogen bonds is very important in quantifying the energetics of hydrogen bond in protein folding.

Theoretical studies based on the standard (nonpolarizable) force fields failed to capture the important features of the hydrogen bond, i.e., polarization which is influenced by local electrostatic environment. Thus the energetic role of hydrogen

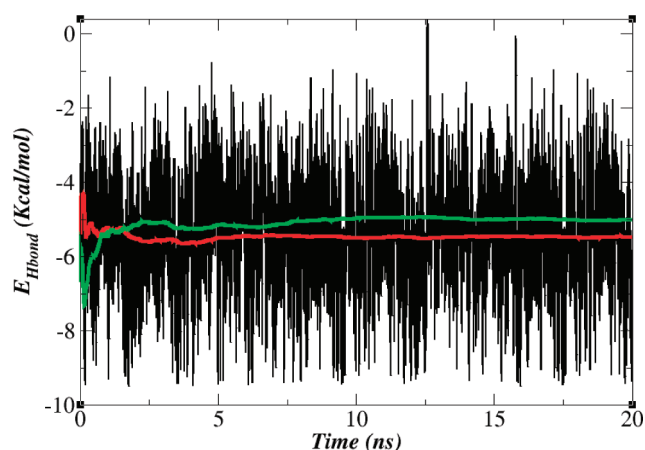


Figure 4. Hydrogen bond energy plotted as a function of simulation time for the wild type (black line). The average H-bond energy of the wild type is shown as a red line. For comparison, the average H-bond energy for the V22A mutant is also shown (green line).

bond formation in protein folding was usually underestimated. Polarized protein-specific charge derived from fragment quantum mechanical calculation of protein in solution provides a practical and reliable means for studying protein dynamics with polarization. The current study underscored the importance of local electrostatic influence on polarization of hydrogen bond. Although the energetic effect of such influence on an individual hydrogen bond may not be very large (less than 1 kcal/mol), the collective effect of all hydrogen bonds in proteins could be significant in protein folding.

COMPUTATIONAL METHODS

The crystal structure of WW domain of PIN determined by Ranganathan et al.²⁶ was used as the starting structure. Polarized protein-specific charge (PPC) has been developed to provide new atomic charges of proteins for better description of protein dynamics near native structure.^{18–21} Fully quantum mechanical calculation of electronic structure of proteins in solution can be achieved through the MFCC²⁷ (molecular fragmentation with conjugated caps) method, in which the protein is partitioned into fragments and the Poisson–Boltzmann equation for protein in solvent is numerically solved.¹⁸ PPC is then derived by fitting atomic charges of protein fragments to their electrostatic potentials calculated for protein native structure in solution. Thus, effective atomic charges of PPC correctly represent the polarized electronic state of the particular protein at a given structure. A detailed description of how the PPC is derived can be found in ref 18.

In the current simulation study, Amber software is used as a computational tool.¹⁶ The protein system is solvated in an octahedron-like TIP3P water box, and the system is neutralized by adding counterions. Periodic boundary conditions and the particle mesh Ewald methods were used to treat long-range electrostatic effects. Each system is relaxed in 5000 steps with constraint on protein, followed by full minimization without any constraints. For the MD simulation, the integration time step is 1 fs. The temperature is regulated using Langevin dynamics with the collision frequency set to 2 ps^{−1}. All of the covalent bonds involving hydrogen atoms are fixed by applying the SHAKE algorithm. After heating and equilibration, the production MD simulation was performed at 300 K (NPT). Two kinds of MD

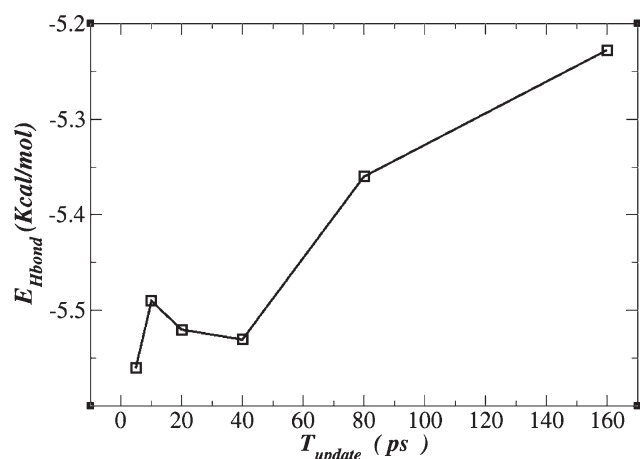


Figure 5. Calculated hydrogen bond (between CO of Arg14 and NH of Tyr23) energy vs charge updating interval.

trajectories were generated for further analysis: (1) a MD simulation with standard Amber99SB force field and (2) a MD simulation with dynamically updated PPC¹⁸ while keeping other parameters of Amber99SB intact.

Although updating the PPC charge every step in the MD simulation is most desirable, quantum chemical calculation to generate PPC for a given protein structure is time-consuming. Thus the proper choice of an updating frequency needs to be tested for practical purposes. In our test calculation, a 16 ns MD simulation was carried out on the wild type PIN WW domain using PPC generated from the crystal structure. The hydrogen bond energy was recalculated with a different frequency of charge updating for the two residues forming the hydrogen bond. The result in Figure 5 shows that a reasonable result is obtained when updating every 40 ps is adopted. A further increase of the updating interval will reduce the reliability of the results.

AUTHOR INFORMATION

Corresponding Author

*E-mail: chicago.ji@gmail.com; john.zhang@nyu.edu.

ACKNOWLEDGMENT

We thank the National Natural Science Foundation of China (Grant Nos. 21003048, 10974054, and 20933002) and Shanghai Pujiang program (09PJ1404000) for financial support. C.G.J. is also supported by “the Fundamental Research Funds for the Central Universities”. We also thank the Computer Center of ECNU for providing us with computational time.

REFERENCES

- (1) Pauling, L.; Delbruck, M. *Science* **1940**, *92*, 77–79.
- (2) Baldwin, R. L. *J. Mol. Biol.* **2007**, *371*, 283–301.
- (3) Bolen, D. W.; Rose, G. D. *Annu. Rev. Biochem.* **2008**, *77*, 339–362.
- (4) Klotz, I. M.; Farnham, S. B. *Biochemistry* **1968**, *7*, 3879–3882.
- (5) Avbelj, F. *J. Mol. Biol.* **2000**, *300*, 1335–1359.
- (6) Avbelj, F.; Baldwin, R. L. *Proc. Natl. Acad. Sci. U.S.A.* **2003**, *100*, 5742–5747.
- (7) Avbelj, F.; Baldwin, R. L. *Proc. Natl. Acad. Sci. U.S.A.* **2004**, *101*, 10967–10972.
- (8) Baldwin, R. L. *J. Biol. Chem.* **2003**, *278*, 17581–17588.

- (9) Yang, A.-S.; Hitz, B.; Honig, B. *J. Mol. Biol.* **1996**, *259*, 873–882.
- (10) Yang, A.-S.; Honig, B. *J. Mol. Biol.* **1995**, *252*, 351–365.
- (11) Yang, A.-S.; Honig, B. *J. Mol. Biol.* **1995**, *252*, 366–376.
- (12) Fernández, A.; Berry, R. S. *Biophys. J.* **2002**, *83*, 2475–2481.
- (13) Fernández, A.; Zhang, X.; Chen, J. In *Progress in Molecular Biology and Translational Science*; Conn, P. M., Ed.; Academic Press: New York, 2008; Vol. 83; pp 53–87.
- (14) Némethy, G.; Steinberg, I. Z.; Scheraga, H. A. *Biopolymers* **1963**, *1*, 43–69.
- (15) Gao, J.; Bosco, D. A.; Powers, E. T.; Kelly, J. W. *Nat. Struct. Mol. Biol.* **2009**, *16*, 684–690.
- (16) Case, D. A.; Cheatham, T. E.; Darden, T.; Gohlke, H.; Luo, R.; Merz, K. M.; Onufriev, A.; Simmerling, C.; Wang, B.; Woods, R. J. *J. Comput. Chem.* **2005**, *26*, 1668–1688.
- (17) Cieplak, P.; Dupradeau, F. Y.; Duan, Y.; Wang, J. M. *J. Phys.-Condensed Matter* **2009**, *21*, 333102.
- (18) Ji, C. G.; Mei, Y.; Zhang, J. Z. H. *Biophys. J.* **2008**, *95*, 1080–1088.
- (19) Ji, C. G.; Zhang, J. Z. H. *J. Am. Chem. Soc.* **2008**, *130*, 17129–17133.
- (20) Ji, C. G.; Zhang, J. Z. H. *J. Phys. Chem. B* **2009**, *113*, 13898–13900.
- (21) Ji, C. G.; Zhang, J. Z. H. *J. Phys. Chem. B* **2009**, *113*, 16059–16064.
- (22) Pace, C. N. *Nat. Struct. Mol. Biol.* **2009**, *16*, 681–682.
- (23) Dill, K. A. *Biochemistry* **1990**, *29*, 7133–7155.
- (24) Pace, C. N.; Hermans, J. *Crit. Rev. Biochem. Mol. Biol.* **1975**, *3*, 1–43.
- (25) Patargias, G. N.; Harris, S. A.; Harding, J. H. *J. Chem. Phys.* **2010**, *132*, 235103.
- (26) Ranganathan, R.; Lu, K. P.; Hunter, T.; Noel, J. P. *Cell* **1997**, *89*, 875–886.
- (27) Zhang, D. W.; Zhang, J. Z. H. *J. Chem. Phys.* **2003**, *119*, 3599–3605.